Supporting Information

The mass of dried nickel foam was measured prior and after electrode deposition. The mass of electrode active material (85% of total mass added) after vacuum drying was calculated as follows:

$$mass_{active\ material} = 0.85 \times (mass_{Ni\ after\ depostion} - mass_{Ni\ before\ deposition}) \quad (1)$$

The specific capacitance C_s from the 2nd discharge half-cycle in the cells was calculated according to Equation 2:[53]

$$C_s = \frac{I \times t}{m \times V} \quad (2)$$

where I is the discharge current, t is the time take by the electrode to discharge, m is the total active mass of the electrode materials in a two- or three-electrode system and V is the potential window during the discharge time.

The energy density, E and the power density, P were calculated according to Equations 3 and 4:[52]

$$E = \frac{1}{2} C \times V^2 \quad (3)$$

$$P = \frac{E}{\Delta t} \quad (4)$$

Where C is the total capacitance, $V$is the potential window, and Δt is the discharge time.

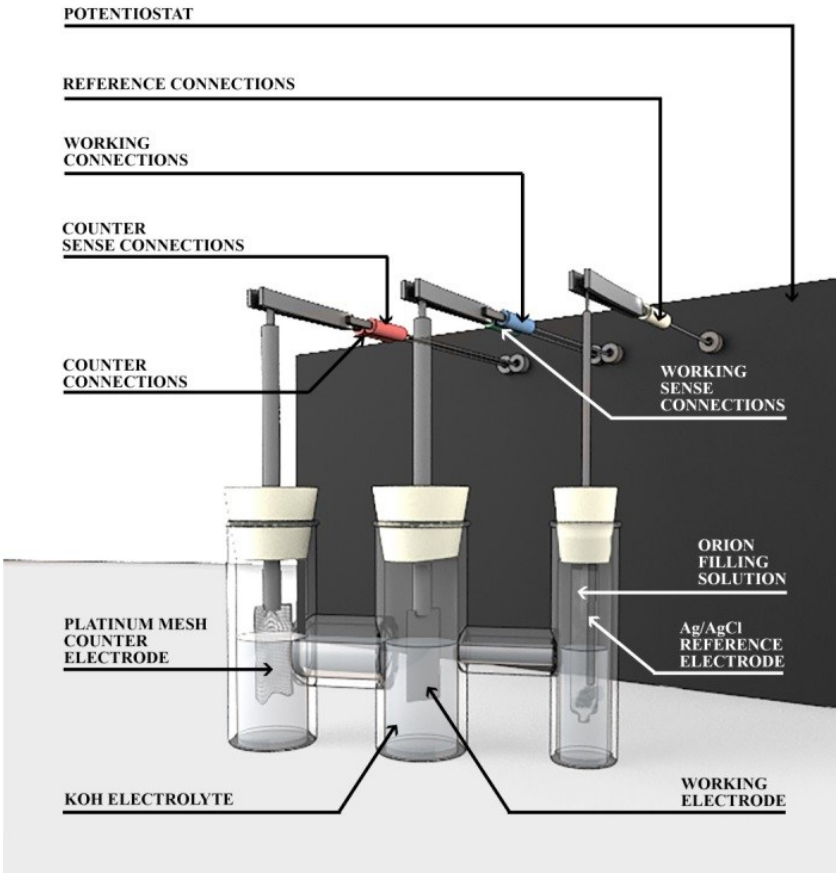

Fig. S1 Schematic diagram of the three-electrode testing system.

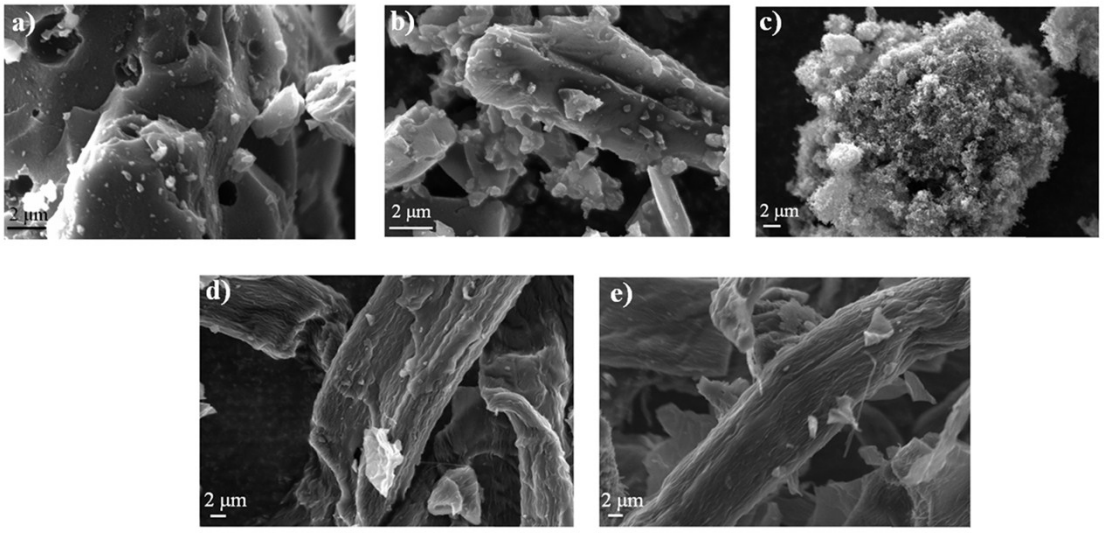

Fig. S2 SEM images of (a) BAC, (b) NAC, (c) KB, (d) carbonized cellulose and (e) KOH-0.005.

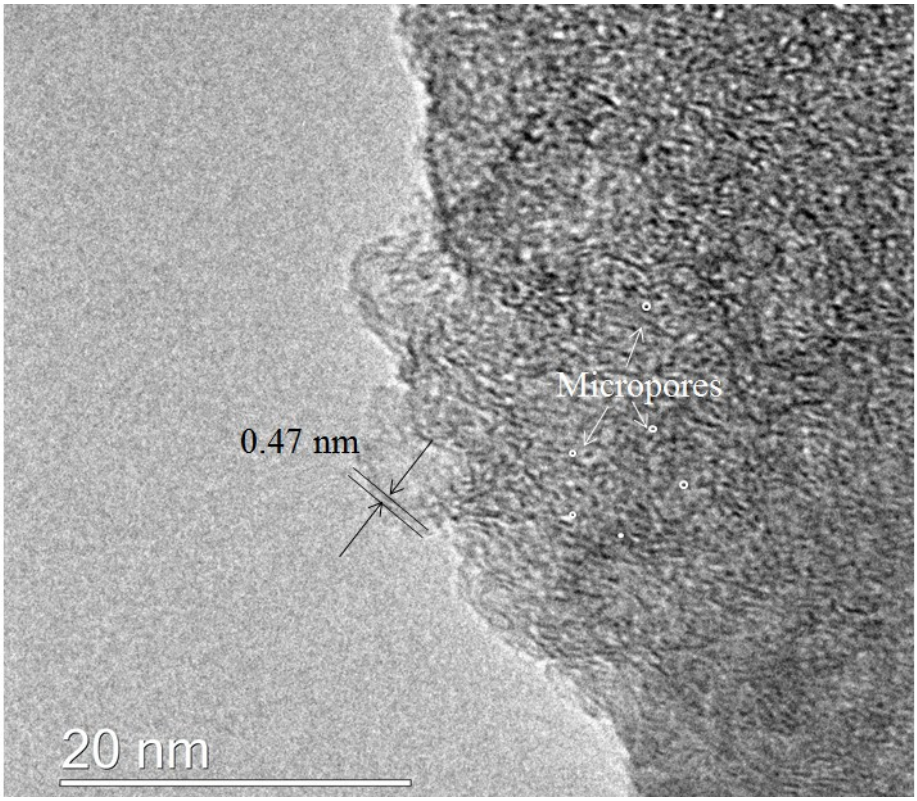

Fig. S3 TEM image of KOH-0.01 showing curved graphene planes (with interlayer spacing higher than that of pristine graphite (0.335 nm)) and formation of micropores due to the carbonization process. Graphitization level depends on precursor carbon material, temperature and heating program during the carbonization process.

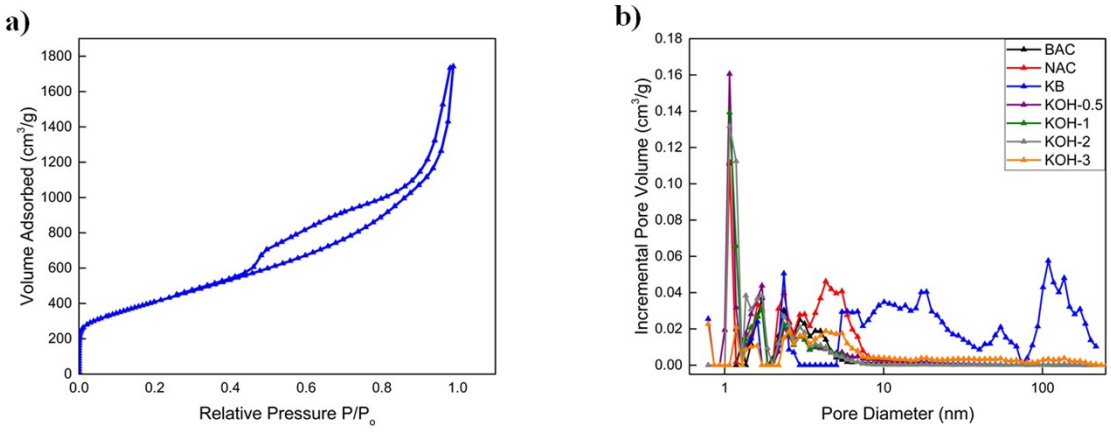

Fig. S4 a) Nitrogen adsorption/desorption isotherm at 77 K of KB and b) incremental pore size distribution of commercial and activated carbons using DFT method.

Table S1: Porous texture identified by CO_2 adsorption isotherms and mercury (Hg) intrusion experiments.

Sample	V(CO_2) (cm^{-3} g^{-1})	V(Hg) (cm^{-3} g^{-1})
CC	0.23	0
KOH – 0.005	0.22	0.008
KOH – 0.01	0.22	0.12
KOH – 0.1	0.28	0.39
KOH – 0.5	0.42	1.01
KOH – 1	0.54	3.45
KOH – 2	0.6	5.17
KOH – 3	0.16	2.21

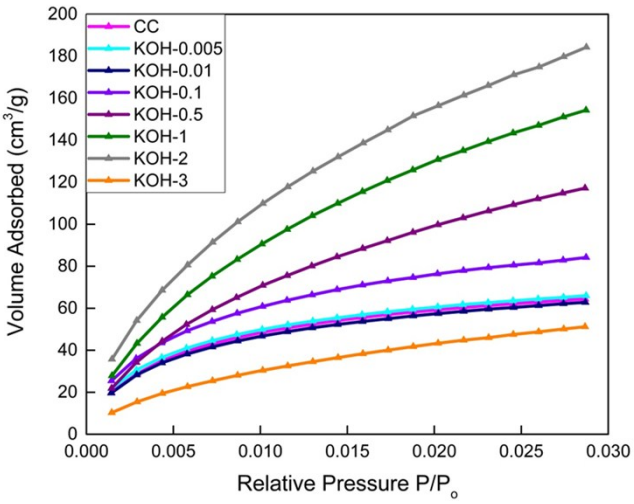

Fig. S5 CO_2 adsorption isotherms at 273 K of all activated samples. The amount of CO2 adsorbed increases with increasing the KOH loading to maximum in KOH-2 sample, beyond which it drastically decreases.

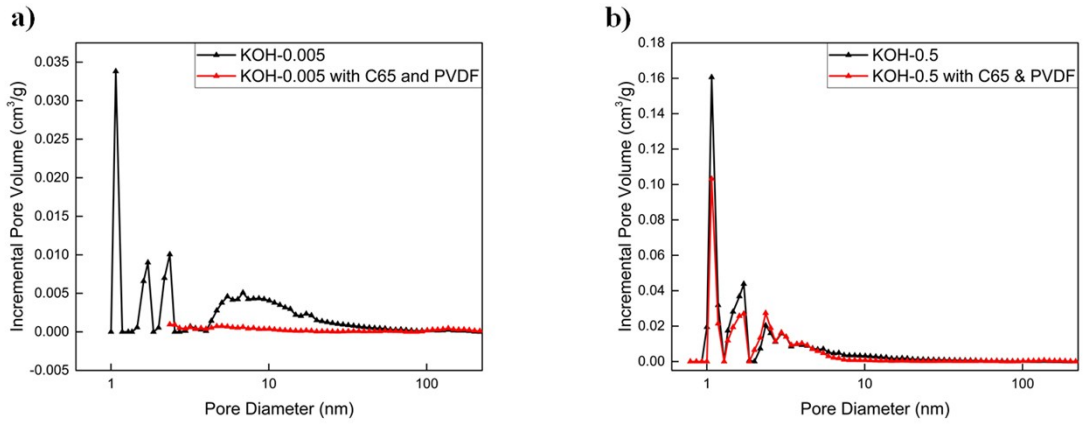

Fig. S6 N_2 adsorption isotherms at 77 K of a) KOH-0.005 sample in comparison with KOH-0.005 sample mixed with PVDF and super C 65 and b) KOH-0.5 sample in comparison with KOH-0.5 sample mixed with PVDF and super C 65.SSA of KOH-0.005 sample dropped from 252 m^2 g^{-1} to 52

m^2 g^{-1}upon the addition of C65 and PVDF. SSA of KOH-0.5 sample decreased to 1063 m^2 g^{-1} from an initial value of 1351 m^2 g^{-1} upon mixing the sample with C65 and PVDF.

Table S2: Elemental analysis of all samples with different KOH loadings showing carbon, hydrogen and oxygen contents.

Sample	Carbon %	Hydrogen %	Oxygen %
CC	90.45	0.63	8.91
KOH – 0.005	89.14	0.77	10.10
KOH – 0.01	86.94	0.90	12.16
KOH – 0.1	79.95	0.80	19.25
KOH – 0.5	72.42	0.87	26.70
KOH – 1	79.62	1.08	19.30
KOH – 2	73.25	1.33	25.42
KOH – 3	71.81	1.15	27.04

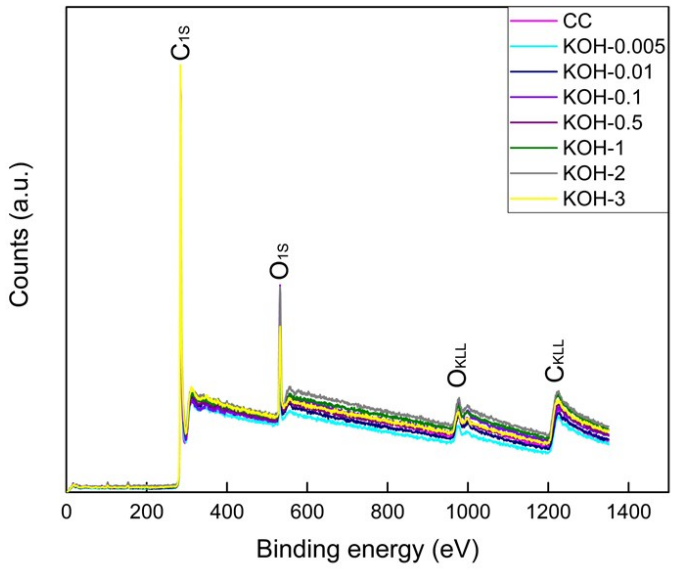

Fig. S7 XPS spectra of all activated samples.

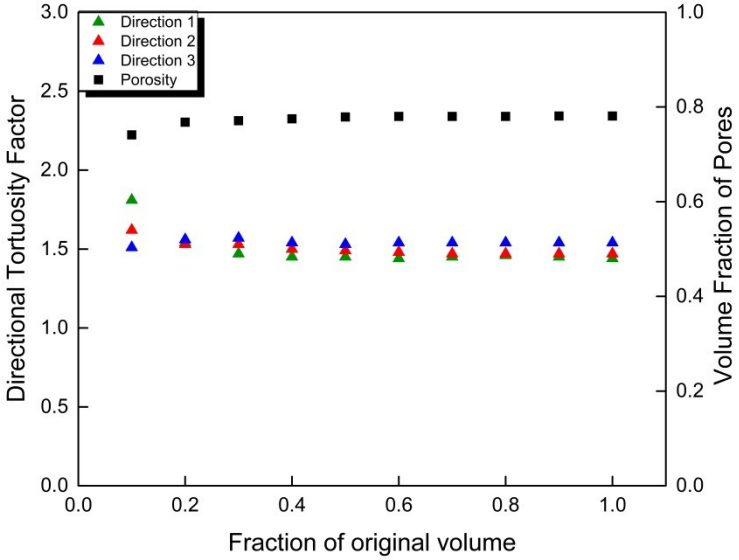

Fig. S8 Representative volume element analysis in the three principal planes (X, Y, Z) for KOH-2 showing that the segmented volumes are considered to be representative volumes for porosity and tortuosity factors of the bulk materials. The directional tortuosities of the sample upon applying the uniform shrinkage analysis confirm that the chosen volume is a representative one as all values converge upon increasing the volume fraction. The porosity evaluated in each of the three planes is of similar value to the calculated one for the segmented volume in Avizo XLab.

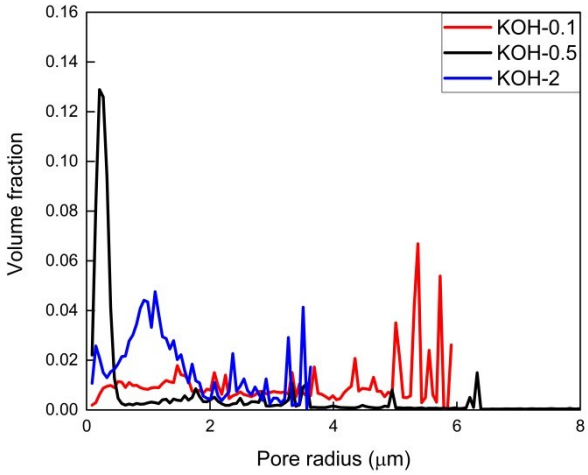

Fig. S9 Continuous pore size distribution of different KOH-activated cellulose samples obtained from all image slices with X-ray tomography technique and determined by the Munch and Holzer 3D method.[31]

The directional tortuosity τ in each of the three planes was calculated feeding the segmented voxel data and reconstructed by Avizo XLab into TauFactor,[38] as follows:

$$\tau = \varepsilon \frac{Q_{cv}}{Q_{pore}} \qquad (5)$$

where ε is the porosity, $Q_{pore}$is the simulated flow rate through the porous network and Q_{cv} is the flow rate through the fully porous control volume.[54]

Representative volume analysis with uniform shrinkage (between 10% and 100% of the total volume element) was then implemented to calculate the characteristic tortuosity factor,τ_c from the tortuosity factors in the three principle directions, due to anisotropy of each of the samples:[38]

$$\tau_c = 3\left(\tau_x^{-1} + \tau_y^{-1} + \tau_z^{-1}\right)^{-1} \qquad (6)$$

where τ_x^{-1}, τ_y^{-1} and τ_z^{-1} are the tortuosity factors in the X, Y and Z principal planes, respectively.

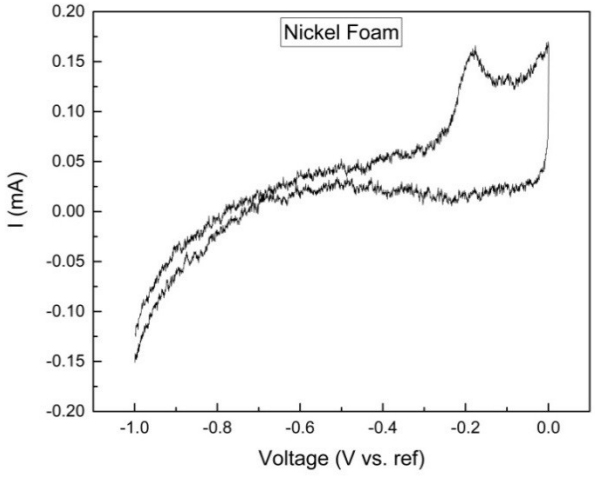

Fig. S10 Cyclic voltammogram if Ni foam at a scan rate of 50 mV s^{-1} in 6 M KOH. The current range is very low in this potential window which proves the minimal effect of current collector on the electrodes' electrochemical performance.

Table S3 Yield percentages of all samples with different KOH loadings upon carbonization at 850 °C in N_2 atmosphere. Yield in general decreases with increasing the KOH/cellulose ratio as the KOH etches the cellulosic materials.

Sample	Yield (%)
Cellulose	10.00
KOH-0.005	12.71
KOH-0.01	13.20
KOH-0.1	12.00
KOH-0.5	10.94
KOH-1	4.03
KOH-2	4.70
KOH-3	1.21

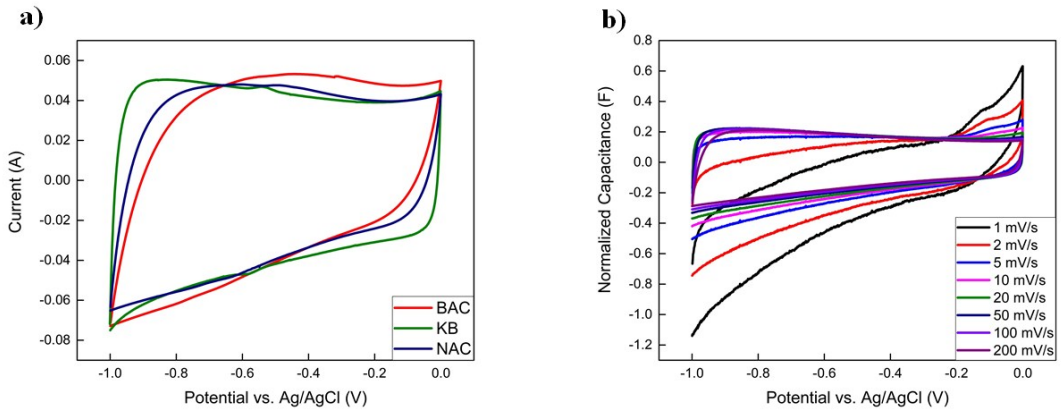

Fig. S11 a) Cyclic voltammograms of commercial materials in three-electrode systems in 6 M KOH at a scan rate of 200 mV s^{-1} and (b) normalized cyclic voltammograms KOH-1 sample in three-electrode system in 6 M KOH at different scan rates ranging from 1 mV s^{-1} to 200 mV s^{-1}.

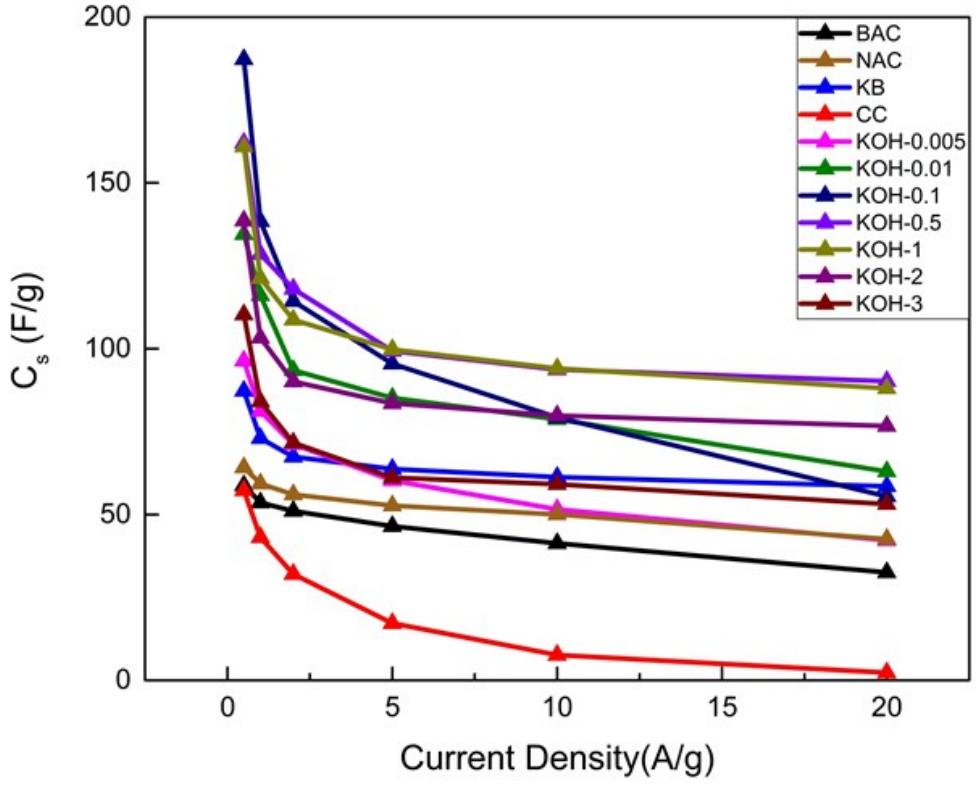

Fig. S12 Capacitance retention of all activated carbons

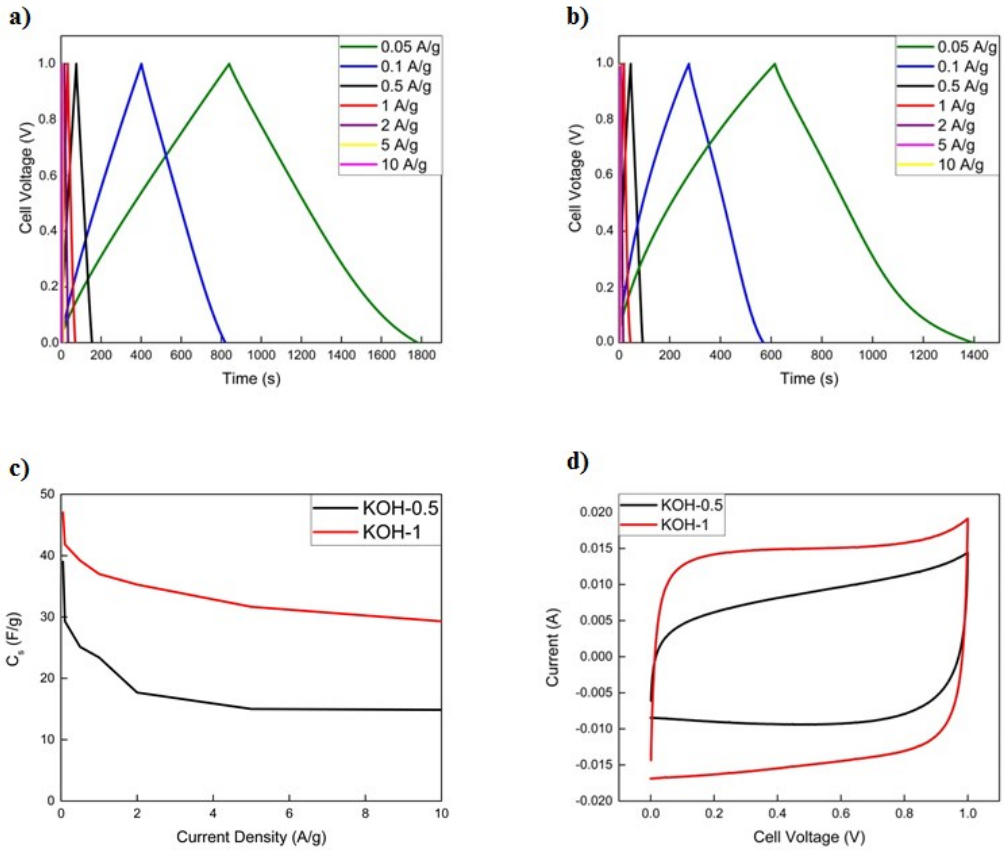

Fig. S13 Two-electrode measurements of symmetrical coin cells in 6 M KOH. Galvanostatic charge-discharge cycles of (a) KOH-1 sample and (b) KOH-0.5 sample at different current densities, (c) capacitance as a function of current density from 0.05 A g^{-1} to 20 A g^{-1}, and (d) cyclic voltammogram of the two coin cells in the potential window 0 − 1 V at 50 mV s^{-1} scan rate.

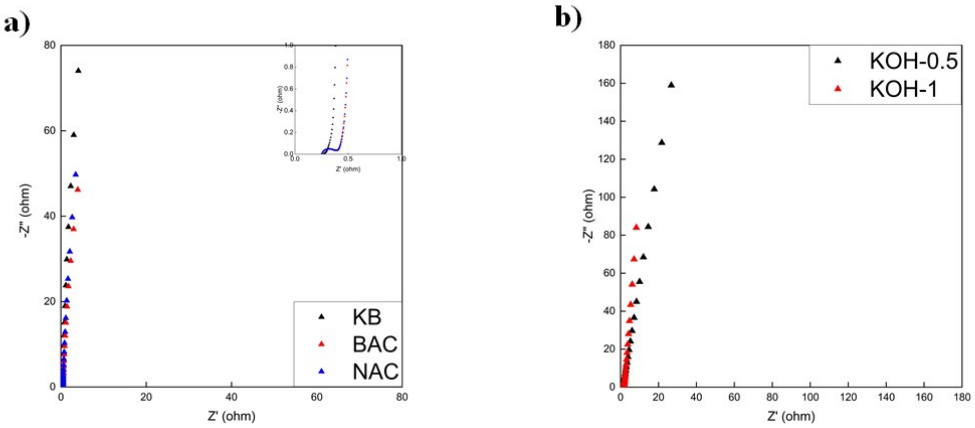

Fig. S14 Nyquist plots in the frequency range of 0.1 Hz to 100 kHz at 0 V vs. open circuit voltage of (a) commercial activated carbons and (b) KOH-0.5 and KOH-1 coin cells.

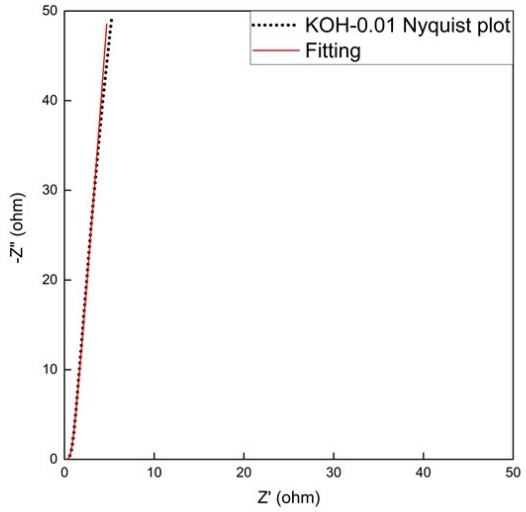

Fig. S15 Nyquist plot of KOH-0.01 sample in three-electrode system with corresponding fitting using the equivalent series circuit.

From the above graph, it is clear that the equivalent circuit fits the electrochemical impedance spectrum of the KOH-activated cellulose sample with goodness of fit value of 1.48×10^{-3}.

Calculations of the different components in the equivalent circuit are tabulated below, whereby the non-ideal capacitance, i.e. the constant phase element (CPE) is calculated according to Equation (7):

$$CPE = C^{\alpha} \qquad (7)$$

where C is the ideal capacitance and α is the non-ideality factor; both of which are evaluated from the fitted curve.